Supporting Information

Proton-Coupled Electron Transfer at Anthraquinone Modified Indium Tin Oxide Electrodes

Caitlin M. Hanna, Andrew Luu, Jenny Y. Yang*

Department of Chemistry, University of California, Irvine, California 92697, United States

Corresponding Author
Email: j.yang@uci.edu

Table of Contents

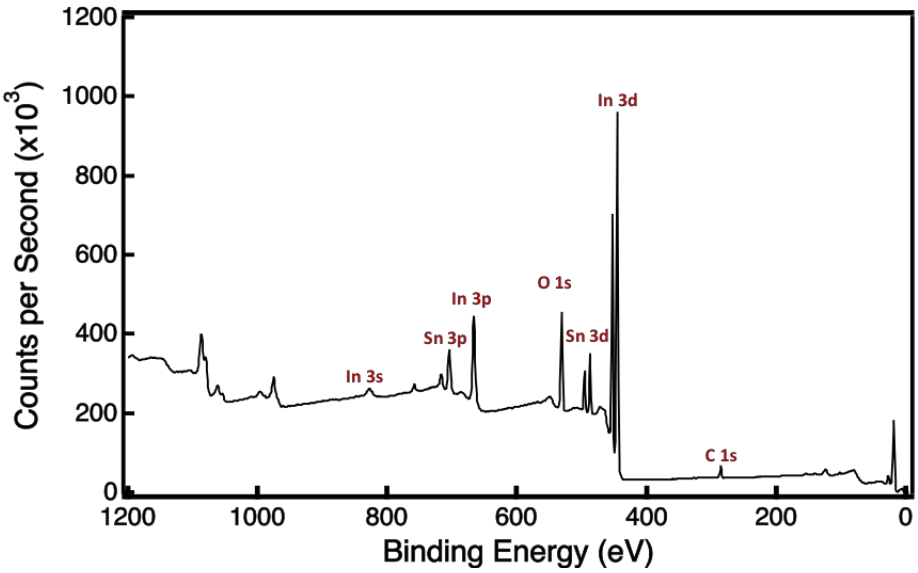

Figure S1. XPS survey spectrum of bare ITO. The features at binding energies higher than 900 eV are attributed to O, In, and Sn Auger peaks.

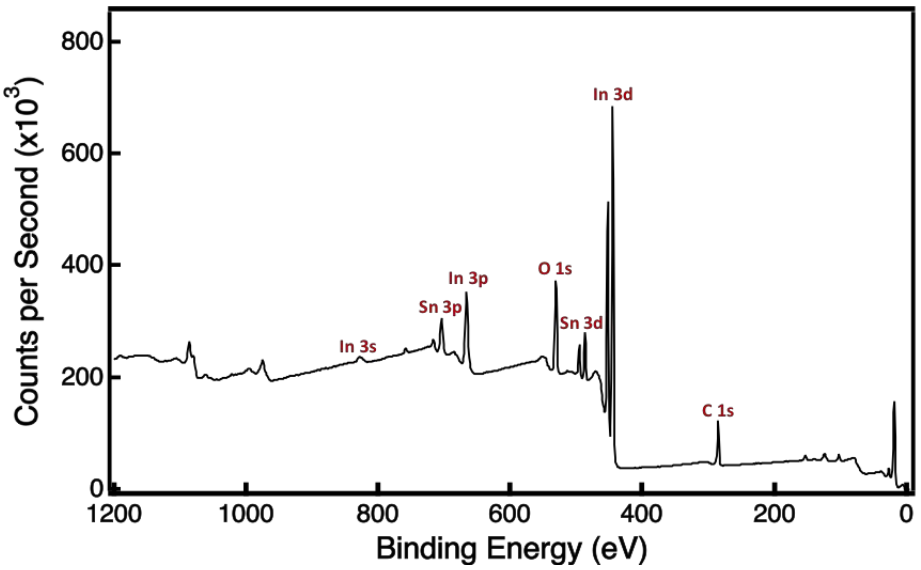

Figure S2. XPS survey spectrum of ITO|Pyr. The features at binding energies higher than 900 eV are attributed to O, In, and Sn Auger peaks.

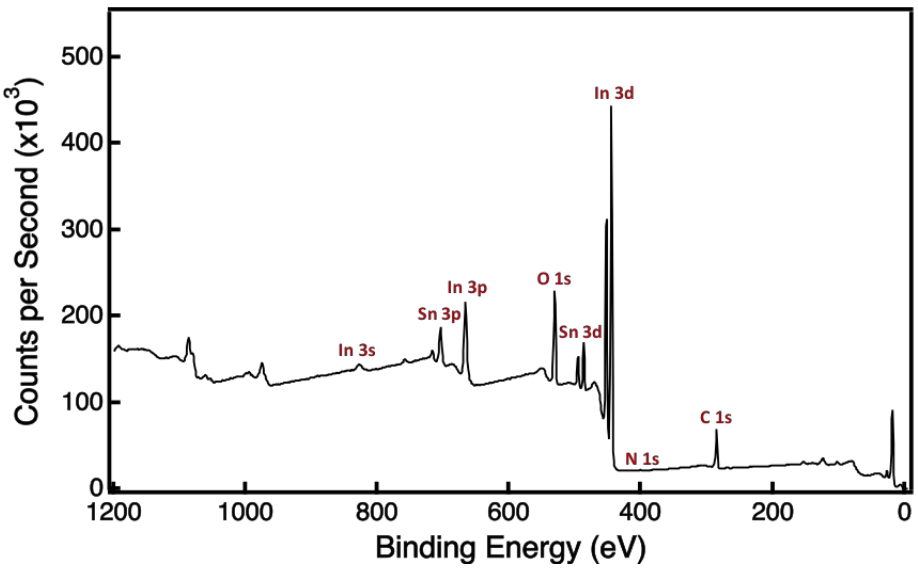

Figure S3. XPS survey spectrum of ITO|Pyr|Pyr(AQ)$_2$. The features at binding energies higher than 900 eV are attributed to O, In, and Sn Auger peaks.

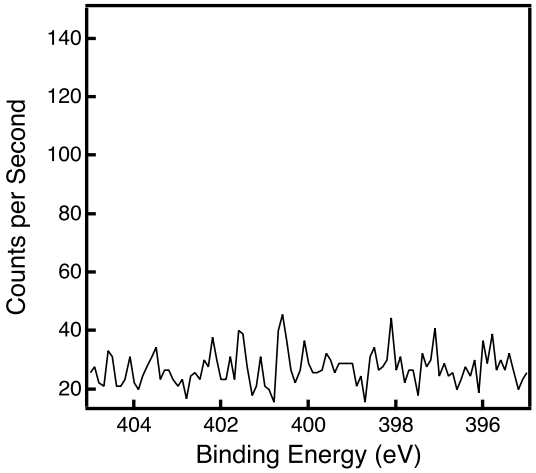

Figure S4. High-resolution XPS spectrum of the N 1s region of bare ITO, exhibiting the expected absence of nitrogen species on the surface.

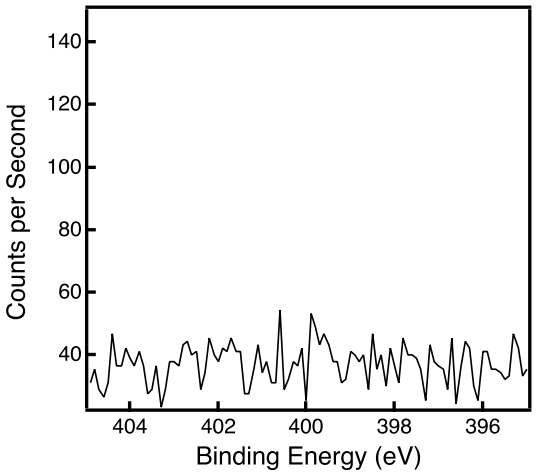

Figure S5. High-resolution XPS spectrum of the N 1s region of ITO|Pyr, exhibiting the expected absence of nitrogen species on the surface.

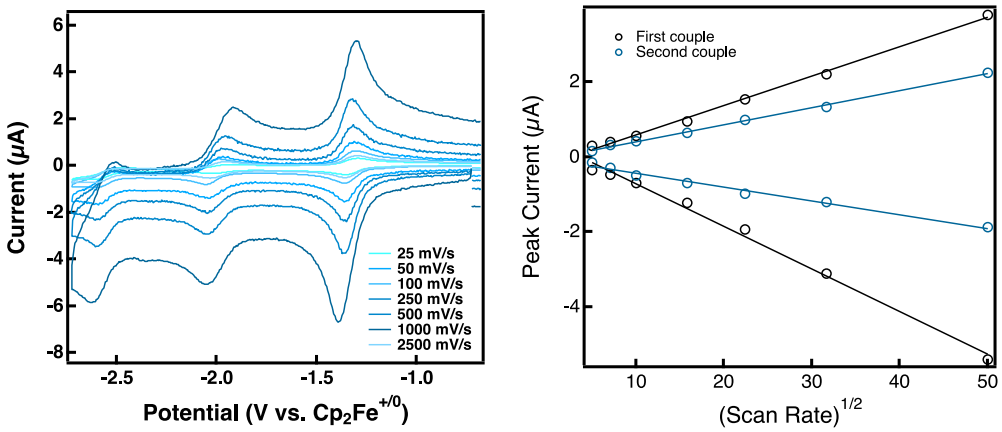

Figure S6. Variable scan rate cyclic voltammetry of $Pyr(AQ)_2$ in dimethylformamide recorded using a glassy carbon disc working electrode, a glassy carbon rod counter electrode, and an Ag^+/Ag pseudo-reference electrode (left) and the corresponding peak current vs. square root of scan rate plot (right).

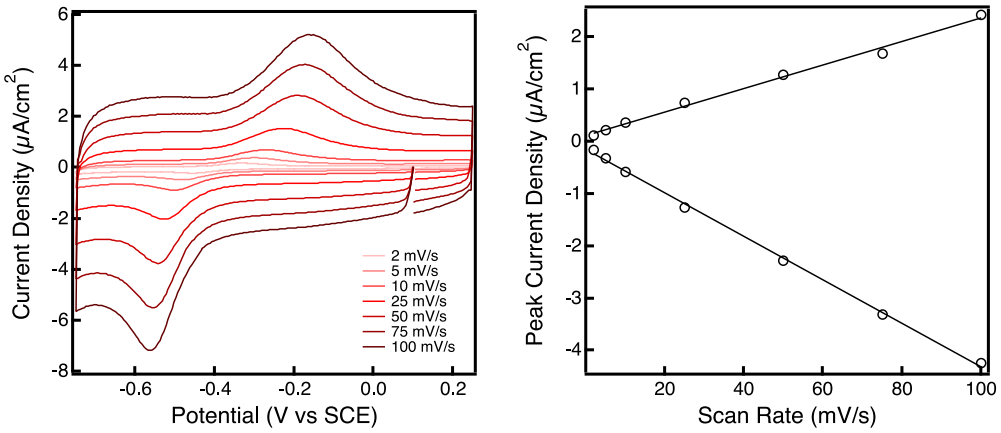

Figure S7. Variable scan rate cyclic voltammetry of ITO|Pyr|Pyr(AQ)$_2$ recorded using a glassy carbon rod counter electrode and an SCE reference electrode at pH 5 (left) and the corresponding peak current density vs. scan rate plot (right).

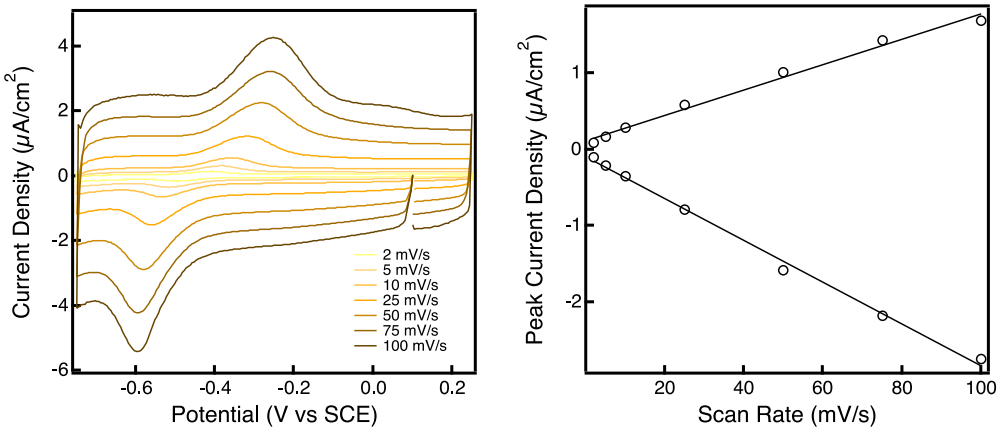

Figure S8. Variable scan rate cyclic voltammetry of ITO|Pyr|Pyr(AQ)$_2$ recorded using a glassy carbon rod counter electrode and an SCE reference electrode at pH 6 (left) and the corresponding peak current density vs. scan rate plot (right).

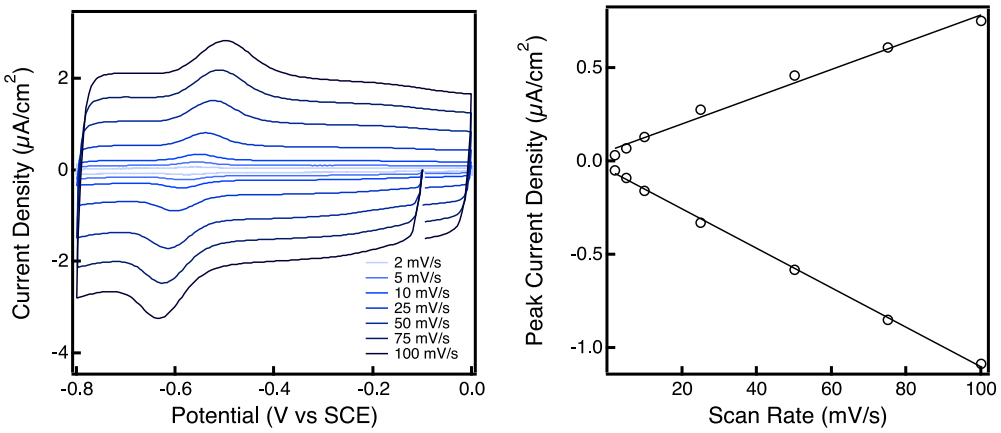

Figure S9. Variable scan rate cyclic voltammetry of ITO|Pyr|Pyr(AQ)$_2$ recorded using a glassy carbon rod counter electrode and an SCE reference electrode at pH 8 (left) and the corresponding peak current density vs. scan rate plot (right).

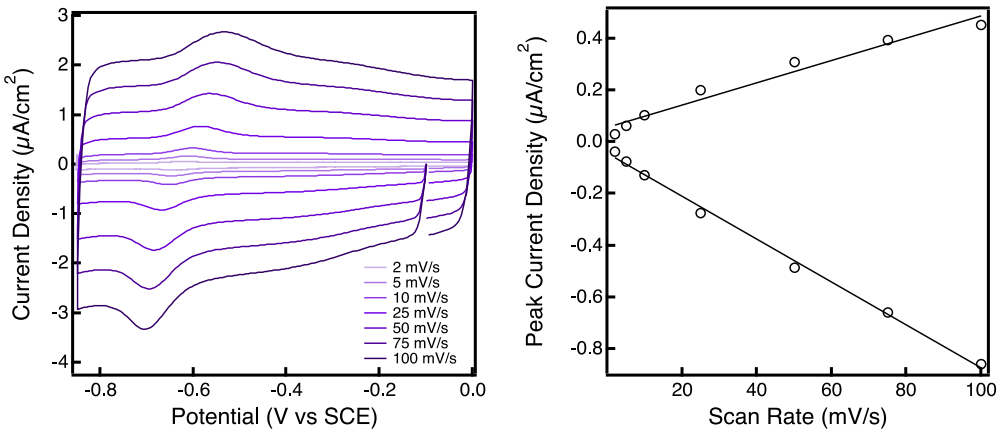

Figure S10. Variable scan rate cyclic voltammetry of ITO|Pyr|Pyr(AQ)$_2$ recorded using a glassy carbon rod counter electrode and an SCE reference electrode at pH 9 (left) and the corresponding peak current density vs. scan rate plot (right).

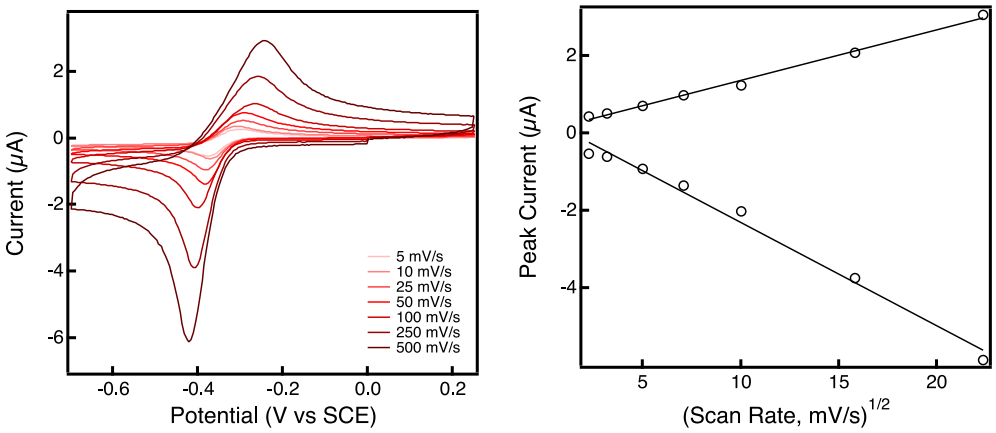

Figure S11. Variable scan rate cyclic voltammetry of AQS in pH 5 citrate buffer recorded using a glassy carbon disc working electrode, a glassy carbon rod counter electrode, and an SCE reference electrode (left) and the corresponding peak current vs. square root of scan rate plot (right).

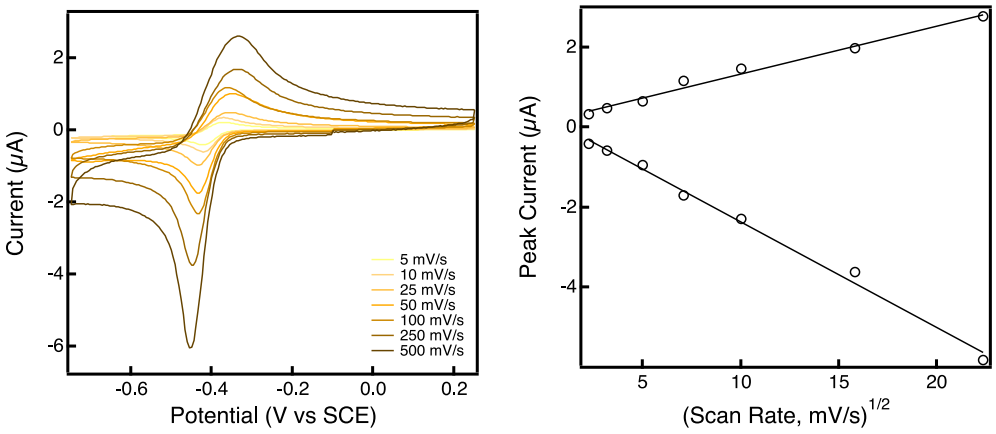

Figure S12. Variable scan rate cyclic voltammetry of AQS in pH 6 citrate buffer recorded using a glassy carbon disc working electrode, a glassy carbon rod counter electrode, and an SCE reference electrode (left) and the corresponding peak current vs. square root of scan rate plot (right).

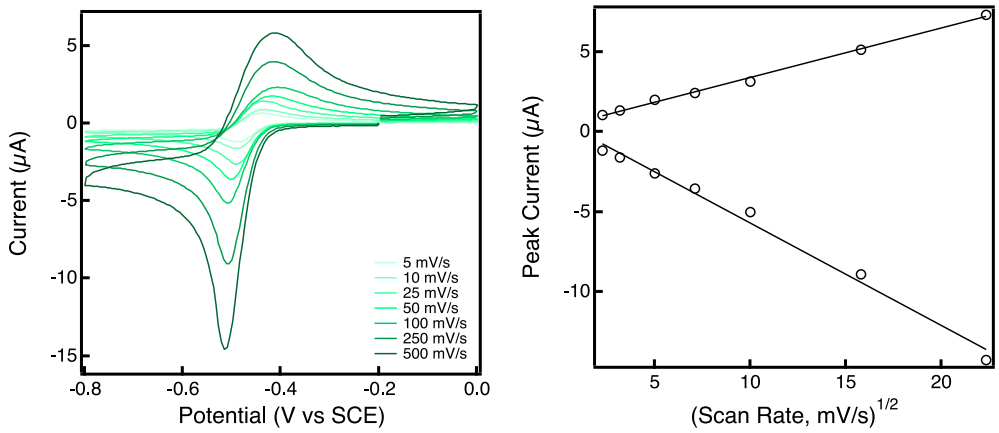

Figure S13. Variable scan rate cyclic voltammetry of AQS in pH 7 HEPES buffer recorded using a glassy carbon disc working electrode, a glassy carbon rod counter electrode, and an SCE reference electrode (left) and the corresponding peak current vs. square root of scan rate plot (right).

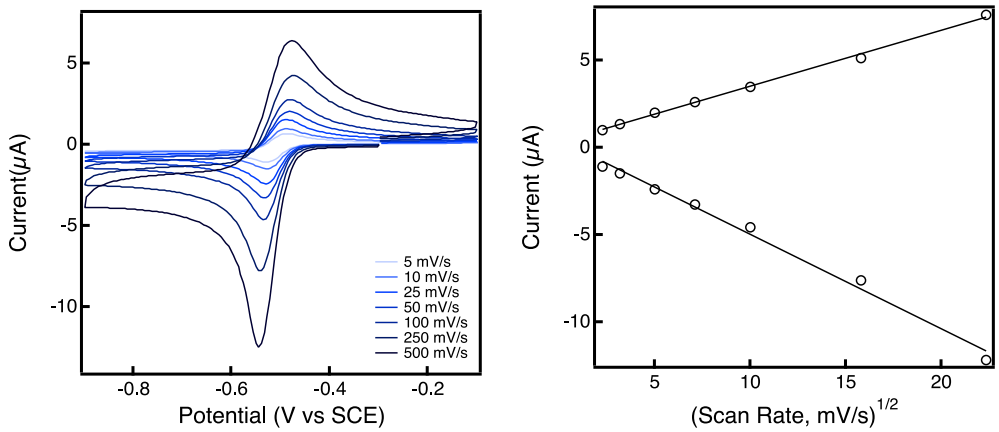

Figure S14. Variable scan rate cyclic voltammetry of AQS in pH 8 HEPES buffer recorded using a glassy carbon disc working electrode, a glassy carbon rod counter electrode, and an SCE reference electrode (left) and the corresponding peak current vs. square root of scan rate plot (right).

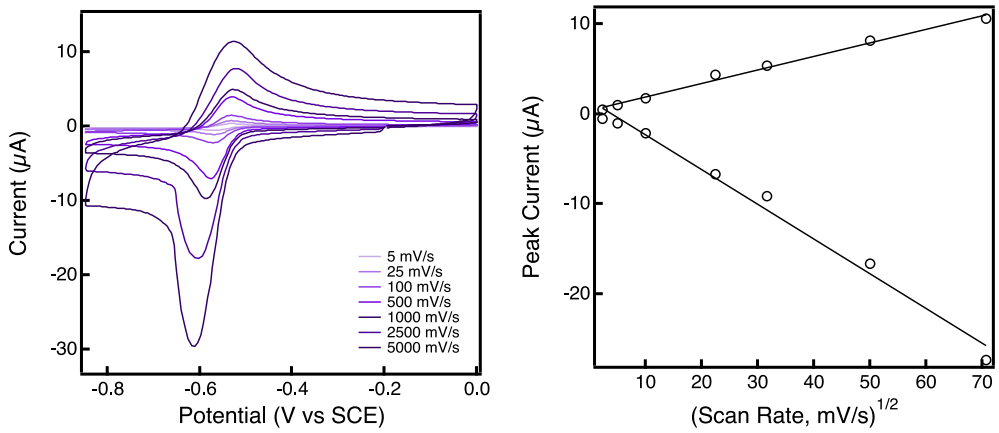

Figure S15. Variable scan rate cyclic voltammetry of AQS in pH 9 borate buffer recorded using a glassy carbon disc working electrode, a glassy carbon rod counter electrode, and an SCE reference electrode (left) and the corresponding peak current vs. square root of scan rate plot (right).

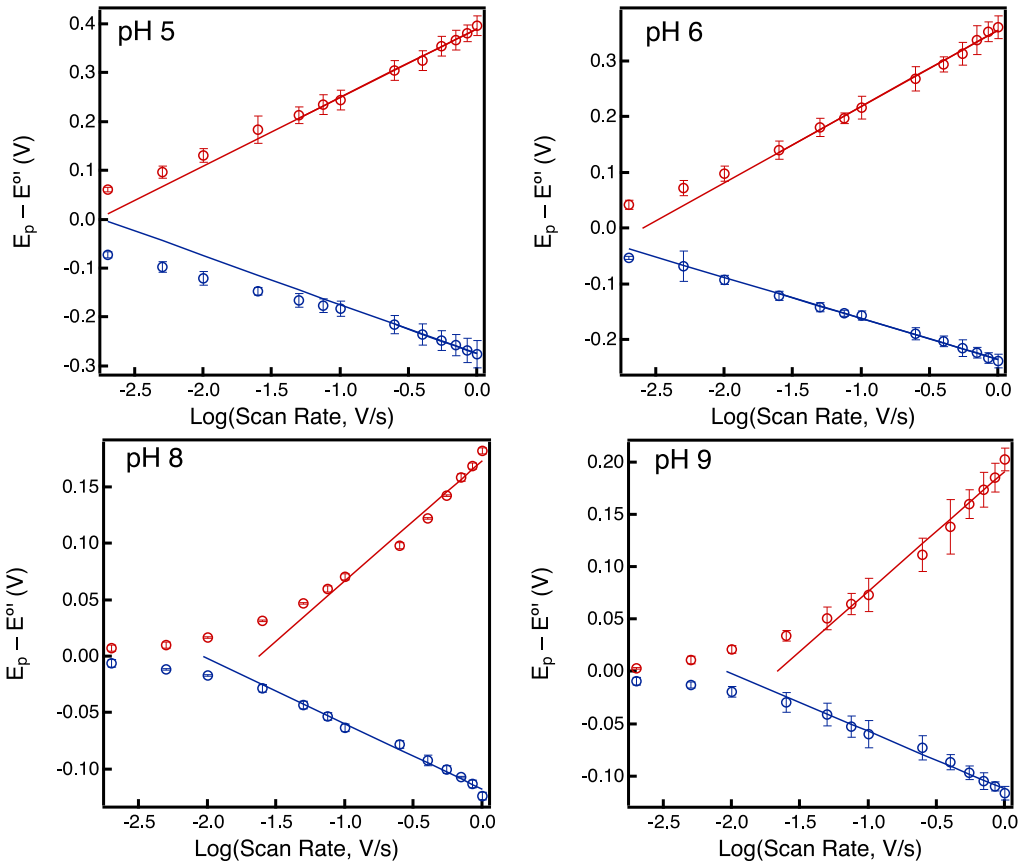

Figure S16. Trumpet plots of ITO|Pyr|Pyr(AQ)$_2$ at pH 5, 6, 8, and 9.

Calculation S1. Sample calculation of k_{app} using the Laviron formalism.[1] Data shown is for an ITO|Pyr|Pyr(AQ)$_2$ electrode at pH 7. Significant figures are taken into account in the final step of the calculation.

Cathodic fit: y = –0.0656x – 0.146
Anodic fit: y = 0.113x + 0.213

Equations (1) and (2) rearranged to reflect the trumpet plot axes:

$$E_{p,c} - E^{\circ\prime} = -\frac{2.3\mathrm{RT}}{\alpha nF}\log\left[\frac{\alpha nFv}{RTk_{app}}\right] \qquad E_{p,a} - E^{\circ\prime} = -\frac{2.3\mathrm{RT}}{(1-\alpha)nF}\log\left[\frac{(1-\alpha)nFv}{RTk_{app}}\right]$$

Where $E_{p,a}$ is the potential of the anodic peak, $E_{p,c}$ is the potential of the cathodic peak, $E^{o\prime}$ is the formal potential calculated by averaging the anodic and cathodic potentials at slow scan rates, v is the scan rate, α is the electron transfer coefficient, k_{app} is the apparent rate constant, R is the ideal gas constant, T is the absolute temperature, F is the Faraday constant, and n is the number of electrons transferred.

Calculation of α and 1– α from slope:

$$Slope_c = \frac{-2.3RT}{\alpha nF} \qquad Slope_a = \frac{-2.3RT}{(1-\alpha)nF}$$

$\alpha = 0.45$ $\qquad$ $1-\alpha = 0.26$

Calculation v_c and v_a from x-intercept:

$$\log(v) = -\frac{y-intercept}{slope}$$

$v_c = 0.013$ V/s $\qquad$ $v_a = 0.0060$ V/s

Calculation of k_{app} using α, 1– α, v_c, and v_a:

$$k_{app,c} = \frac{\alpha nFv_c}{RT} \qquad k_{app,a} = \frac{(1-\alpha)nFv_a}{RT}$$

$k_{app,c} = 0.2\ s^{-1}$ $\qquad$ $k_{app,a} = 0.3\ s^{-1}$

Reported k_{app} values are given as averages of $k_{app,c}$ and $k_{app,a}$ across three individually prepared samples and error is reported as the standard deviation from the mean.

Calculation S2. Sample calculation of k_{app} using the Kochi method. Data shown is for the cyclic voltammetry of AQS dissolved in pH 7 HEPES buffer at 50 mV/s. Significant figures are taken into account in the final step of the calculation.

α is first determined from the slope of the linear portion (irreversible region) of the plot of $E_{p,c}$ vs. log(v) (See Figure S17) using the following equation:[2]

$$\alpha = \left[\frac{1}{slope}\right]\left[\frac{2.3RT}{2nF}\right]$$

$\text{Slope}_{\text{pH 7}} = 0.057$

$\alpha_{\text{pH 7}} = 0.26$

k_{app} is then calculated at multiple scan rates in the irreversible region and reported as an average across all scan rates using the following equation:[2]

$$k_{app} = 2.18\left[\frac{\alpha DnFv}{RT}\right]^{1/2} exp\left[\frac{-\alpha^2 nF(E_{p,a} - E_{p,c})}{RT}\right]$$

Where $E_{p,a}$ is the potential of the anodic peak, $E_{p,c}$ is the potential of the cathodic peak, v is the scan rate, α is the electron transfer coefficient, k_{app} is the apparent rate constant, D is the diffusion coefficient calculated using the Randles-Sevcik equation, R is the ideal gas constant, T is the absolute temperature, F is the Faraday constant, and n is the number of electrons transferred.

Error is reported as the standard deviation from the average across all scan rates.

Table S1. k_{app} values determined using the Kochi method for AQS at pH 7 across various scan rates.

Scan Rate (V/s)	$E_{p,a} - E_{p,c}$ **(V)**	k_{app} **(cm/s)**
0.25	0.088	0.017
0.5	0.104	0.023
0.75	0.184	0.018
1	0.166	0.023
1.5	0.197	0.024
2.5	0.207	0.029
5	0.260	0.031
10	0.272	0.042
Average	N/A	0.03
Standard Deviation	N/A	0.01

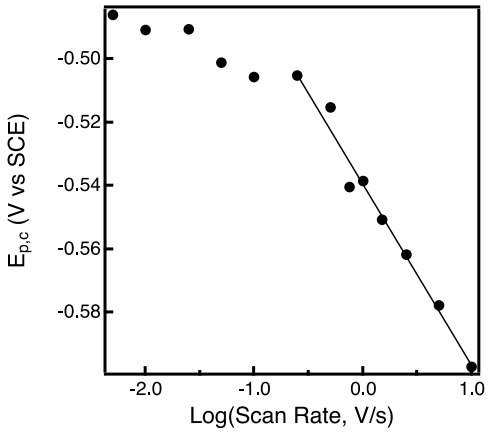

Figure S17. Plot of $E_{p,c}$ vs. log(scan rate) for AQS in pH 7 HEPES buffer.

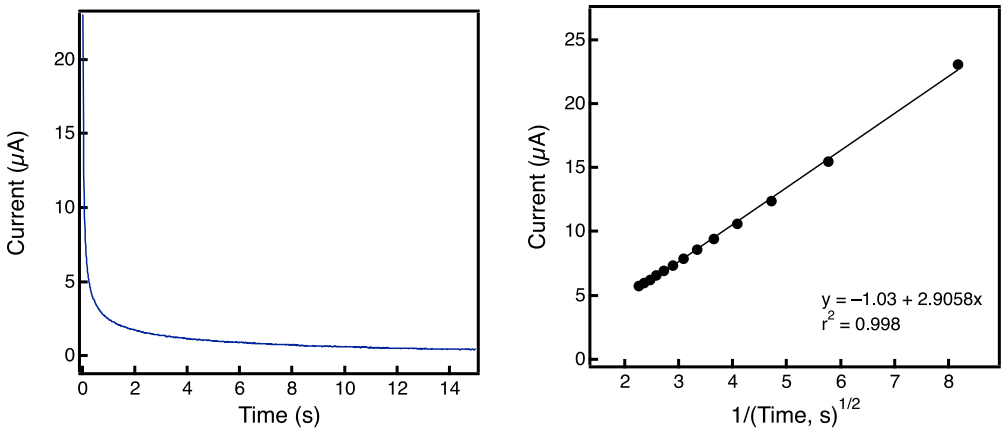

Figure S18. Representative current vs. time plot (left) and linear fit (right) from chronoamperometry of a 1 mM $Fe(C_5H_5)_2$ solution used to determine electroactive surface area of a 1 mm diameter glassy carbon electrode (geometric surface area = 0.0079 cm^2).

Table S2. Data for chronoamperometry of a $Fe(C_5H_5)_2$ solution used to determine electroactive surface area of a 1 mm diameter glassy carbon electrode.

Trial	**Slope of fit of current vs. (time, s)$^{1/2}$ (x 10^{-6})**	**Calculated electroactive area (cm^2) (x 10^{-2})**
1	2.91	1.09
2	2.95	1.11
3	2.98	1.12
4	2.92	1.10
5	2.92	1.11
Average	N/A	1.10

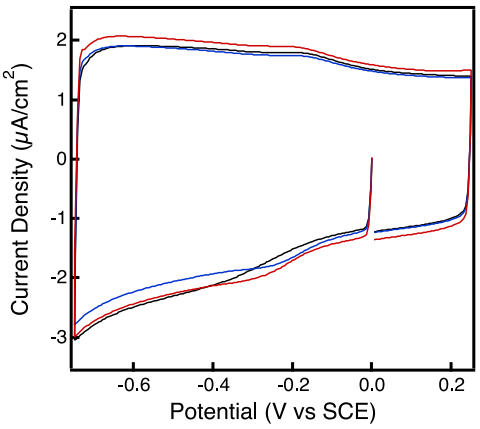

Figure S19. Cyclic voltammograms of ITO recorded using a glassy carbon rod counter electrode and an SCE reference electrode in pH 7 phosphate buffer. All three voltammograms were recorded using the same working electrode.

References

1. Laviron, E., The Use of Linear Potential Sweep Voltammetry and of A.C. Voltammetry for the Study of the Surface Electrochemical Reaction of Strongly Adsorbed Systems and of Redox Modified Electrodes. *J. Electroanal. Chem. Interfacial Electrochem.* **1979,** *100*, 263.

2. Klingler, R. J.; Kochi, J. K., Electron-Transfer Kinetics from Cyclic Voltammetry. Quantitative Description of Electrochemical Reversibility. *J. Phys. Chem.* **1981,** *85*, 1731.